

Photocurrent, Rectification, and Magnetic Field Symmetry of Induced Current through Quantum Dots

L. DiCarlo and C. M. Marcus

Department of Physics, Harvard University, Cambridge, Massachusetts 02138, USA

J. S. Harris, Jr.

Department of Electrical Engineering, Stanford University, Stanford, California 94305, USA

(Received 16 April 2003; published 11 December 2003)

We report mesoscopic dc current generation in an open chaotic quantum dot with ac excitation applied to one of the shape-defining gates. For excitation frequencies large compared to the inverse dwell time of electrons in the dot (i.e., GHz), we find mesoscopic fluctuations of induced current that are fully *asymmetric* in the applied perpendicular magnetic field, as predicted by recent theory. Conductance, measured simultaneously, is found to be symmetric in field. In the adiabatic (i.e., MHz) regime, in contrast, the induced current is always symmetric in field, suggesting its origin is mesoscopic rectification.

DOI: 10.1103/PhysRevLett.91.246804

PACS numbers: 73.23.-b, 78.70.Gq

The study of phase-coherent electron transport in systems with rapidly time-varying potentials significantly extends the domain of mesoscopic physics, and is likely to be important in quantum information processing in the solid state, where gate operations must be fast compared to decoherence rates. Three regimes of transport where quantum interference effects play an important role may be identified: dc transport with static potentials, exhibiting coherence effects such as universal conductance fluctuations (UCF) and weak localization; adiabatic transport, showing mesoscopic rectification and charge pumping [1–7]; and high-frequency transport, where photovoltaic effects [8–15] and decoherence from a fluctuating electromagnetic environment have been studied [16–19]. Recently, theory connecting these regimes in quantum dots has appeared [20–23], with most predicted effects remaining unexplored experimentally.

In this Letter, we compare dc currents induced by adiabatic and nonadiabatic sinusoidal modulation of the voltage on one of the confining gates of an open GaAs/AlGaAs quantum dot. Motivated by recent theory [5,7,21], we pay particular attention to the symmetry of the induced dc current as a function of perpendicular magnetic field, B . For adiabatic frequencies ($\omega \ll \tau_d^{-1}$, where τ_d is the dwell time of electrons in the dot) mesoscopic fluctuations (about a zero average) of induced current are always found to be symmetric in B . As discussed in [7,24], this suggests *rectification*—due to coupling of the gate voltage to the reservoirs combined with gate-dependent conductance—as the principal source of induced current in this regime. On the other hand, for gate-voltage modulation at GHz frequencies ($\omega \gtrsim \tau_d^{-1}$), the induced dc current may be either predominantly symmetric or completely asymmetric in B , depending on the particular frequency.

We interpret these results as showing competing mechanisms of induced mesoscopic current in the GHz

regime, with photocurrent producing a signal asymmetric in B and rectification producing a signal symmetric in B . Full asymmetry of photocurrent reflects the broken time-reversal symmetry due to the ac excitation. In contrast, rectification arises from a modulated conductance, which remains predominantly symmetric in field even when an ac excitation is present. Which effect dominates depends strongly on the frequency of the modulation. We thus establish field symmetry as an experimental tool for separating these different physical effects. This allows us to study, for instance, how rectification and photocurrent separately depend on the amplitude of the applied ac modulation.

The quantum dot investigated was formed by electrostatic gates 90 nm above the two-dimensional electron gas (2DEG) in a GaAs/AlGaAs heterostructure, and has an area $A \sim 0.7 \mu\text{m}^2$, accounting for ~ 50 nm depletion at the gate edge. The bulk density of the 2DEG was $2 \times 10^{11} \text{cm}^{-2}$ and the mobility $1.4 \times 10^5 \text{cm}^2/\text{Vs}$, giving a bulk mean free path $\sim 1.5 \mu\text{m}$. Ohmic contact resistances were on the order of 350Ω . Measurements are presented for the case of one fully conducting (spin degenerate) mode per lead, which gives an average dot conductance $\langle g \rangle \sim e^2/h$. Relevant time scales include the dot crossing time $\tau_{\text{cross}} \sim \sqrt{A}/v_F \sim 4 \text{ps}$ and dwell time within the dot $\tau_d = h/2\Delta \sim 0.2 \text{ns}$ for single-mode leads ($\Delta = 2\pi\hbar^2/m^*A \sim 10 \mu\text{eV}$ is the quantum level spacing, v_F is the Fermi velocity and m^* the effective electron mass).

The induced dc current through the dot was measured in a dilution refrigerator via 300Ω leads, while two semirigid 50Ω coaxial lines allowed ac excitation to be coupled from the high-frequency source (Wiltron 6769B) to either of two gates of the dot over a range 10 MHz to 20 GHz. A room temperature bias tee enabled ac and dc voltage to be simultaneously applied to the chosen gate. With coaxial lines attached, the base electron temperature, where all measurements were carried out, was

~ 200 mK, determined from UCF amplitude [17] and Coulomb blockade peak widths [25]. The ac excitation was chopped at 153 Hz by a square pulse of variable duty cycle, p (given as a percentage). The induced current was amplified with an ac-coupled Ithaco 1211 current amplifier (nominal input impedance 2 k Ω) and lock-in detected. Conductance was simultaneously measured by applying a 17 Hz, $2 \mu\text{V}_{\text{rms}}$ sinusoidal voltage bias across the dot. Output of the same current amplifier was then detected using a second lock-in at 17 Hz. The measured conductance g_p was found to be a simple weighted average of the conductance with excitation on (g_{on}) and off (g_{off}), $g_p \approx pg_{\text{on}} + (1-p)g_{\text{off}}$, as seen in Fig. 1(d).

Figures 1(a) and 1(b) show dot conductance $g_{50}(\pm B)$ and induced current $I(\pm B)$, with $p = 50\%$ duty cycle, as a function of perpendicular field, B , for applied frequencies of 10 MHz ($\omega\tau_d \sim 0.01$) and 5.56 GHz ($\omega\tau_d \sim 7$). Dot conductances are in all cases found to be symmetric in B , and show the expected weak localization dip at $B = 0$ and UCF. The induced current with 10 MHz excitation is also symmetric in field. In contrast, the induced current for 5.56 GHz applied to the gate is found to be fully asymmetric in field. This is evident in the traces in Fig. 1(b). The difference between induced current at 10 MHz and 5.56 GHz is seen most clearly by looking at the correlation between induced currents at $\pm B$, defined by $C_I(B) = [\delta I(B)\delta I(-B)]/\langle \delta I(B)^2 \rangle_B$. The brackets denote an average over the measured magnetic field range, and δI is the deviation of the current from its average value over this range. For 10 MHz, C_I is non-negative for all magnetic field values, whereas for 5.56 GHz it changes sign numerous times.

The correlation field scales of mesoscopic fluctuations of induced current and conductance for 10 MHz and 5.56 GHz are roughly equivalent, ~ 1.5 mT, as determined from slopes of log-power spectra [26]. Induced dc current at 10 MHz (5.56 GHz) have roughly zero average and rms fluctuation amplitude of ~ 20 (13) pA corresponds to ~ 12 (0.015) electrons per cycle. These values are obtained for ac gate voltages of 6.4 (~ 12) mV $_{\text{rms}}$, comparable to the measured dc gate-voltage correlation scale, ~ 10 mV. (The ac gate voltage at 10 MHz was calibrated and found to be equal to the voltage applied at the top of the cryostat; the ac gate voltage at 5.56 GHz could not be easily calibrated and instead was estimated by locating the inflection of the curve of induced dc current versus incident power, as seen for instance in Fig. 3(d), and comparing to theory [21].)

Figure 2 shows fluctuations of conductance and induced current as a function of the dc gate voltage, V_g^{dc} , on a shape distorting gate of the dot—the same gate to which the ac excitation is applied—at opposite magnetic field values, ± 50 mT. The conductance traces $g(V_g^{\text{dc}})$ in Fig. 2(a) are nearly identical at ± 50 mT, for both 10 MHz and 2.4 GHz excitations. Induced current fluctuations, shown in Fig. 2(b), are symmetric at 10 MHz, but are not symmetric for 2.4 GHz.

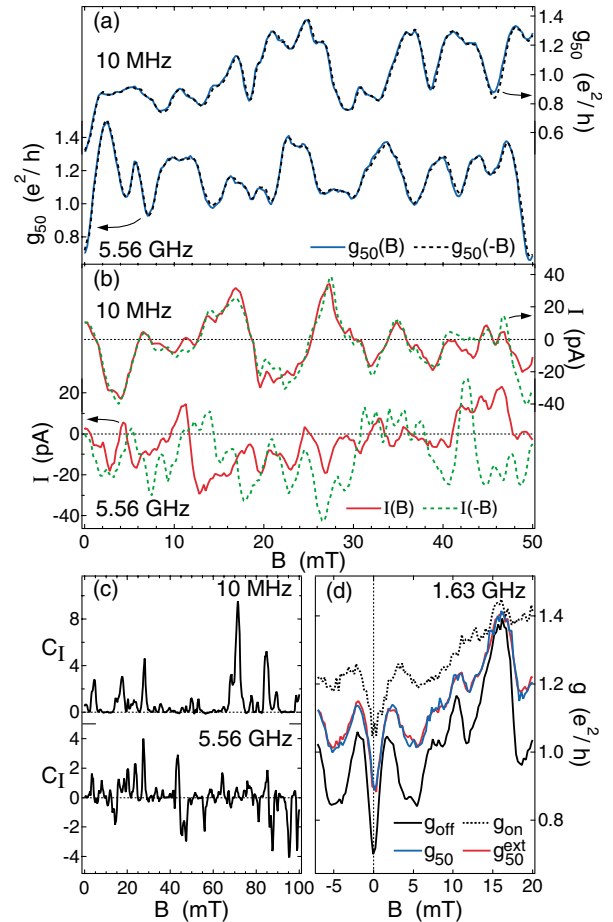


FIG. 1 (color). (a) Conductance $g_{50}(\pm B)$ as a function of perpendicular magnetic field B , for 200 nW of incident radiation at 10 MHz (top) and 370 nW at 5.56 GHz (bottom). (b) Induced dc currents $I(\pm B)$, measured simultaneously with the conductance traces in (a). (c) Cross correlation $C_I(B)$ (see text) of induced current fluctuations at $\pm B$. Correlation is everywhere nonnegative for 10 MHz, but both positive and negative for 5.56 GHz. (d) Comparison of measured dot conductance with 50% duty cycle, g_{50} (blue), and extracted trace $g_{50}^{\text{ext}} = (g_{\text{off}} + g_{\text{on}})/2$ (red), an average of traces with ac excitation off, g_{off} (black), and excitation on, g_{on} (dashed). Traces at different frequencies were made for different dot shape configurations, and hence are uncorrelated.

Using the *same* gate both to drive the dot at ac and change dot shape as a slowly swept parameter allows the induced dc current to be compared to a simple model of rectification [7,24] applicable in the adiabatic limit. The model takes the measured $g(V_g^{\text{dc}})$ as input, and assumes that the ac part of the total gate voltage, $V_g(t) = V_g^{\text{dc}} + V_g^{\text{ac}} \sin(\omega t)$, couples to the source and drain reservoirs of the dot, giving rise to a (possibly phase shifted) drain-source voltage, $V_{ds}(t) = \alpha V_g^{\text{ac}} \sin(\omega t + \phi)$, with α and ϕ as parameters. The dc rectification current resulting from $V_{ds}(t)$ and $g[V_g(t)]$ is given by

$$I_{\text{rect}} = \frac{\omega}{2\pi} \int_0^{2\pi/\omega} \alpha V_g^{\text{ac}} \sin(\omega t + \phi) g[V_g(t)] dt. \quad (1)$$

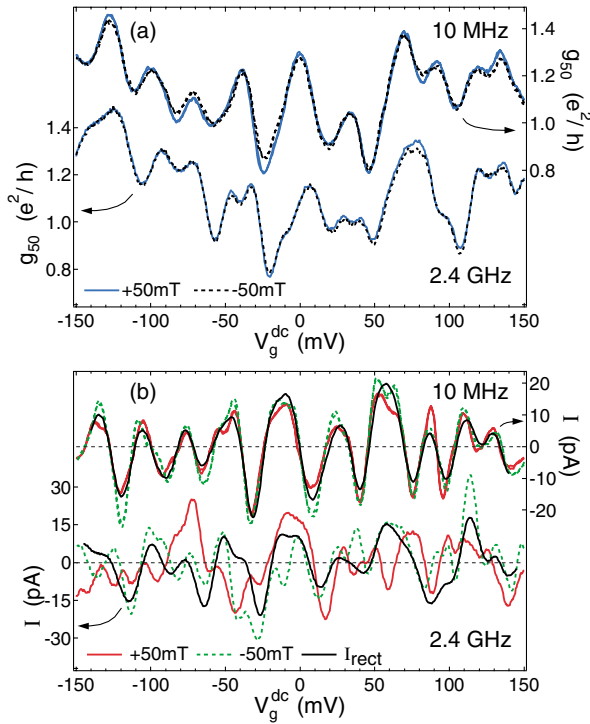


FIG. 2 (color). (a) Conductance as a function of the dc voltage on the same gate to which ac is coupled, at +50 mT and -50 mT, for 115 nW of incident power at 10 MHz (top) and 45 nW at 2.4 GHz (bottom). Two traces are shown at each magnetic field for 10 MHz, revealing the degree of repeatability in the measurements. Traces at different frequencies were taken on different days. (b) Simultaneous measurements of induced dc currents. Currents calculated using the rectification model are also shown, in black, for numerical parameters given in the text.

For V_g^{ac} much less than the gate-voltage correlation scale, $I_{\text{rect}} \approx \frac{\alpha}{2} \cos(\phi) (V_g^{\text{ac}})^2 (dg/dV_g)$ [7]. However, for the data in Fig. 2, $V_g^{\text{ac}} = 6.8 \text{ mV}$ ($\sim 8 \text{ mV}$) for 10 MHz (2.4 GHz), which is not much smaller than the correlation voltage of 10 mV, so the full integral, Eq. (1), is used to model rectification. Figure 2(b) shows a comparison of measured currents and rectification currents calculated from Eq. (1), using the +50 mT data from Fig. 1(a) as input and values $\alpha = 7(6) \times 10^{-4}$ and $\phi = 0(0)$ for 10 MHz (2.4 GHz). For the 10 MHz data, the similarity between the model and the measured current suggests that rectification adequately accounts for the induced current. On the other hand, the induced dc current at 2.4 GHz ($\omega\tau_d \sim 3$) does not appear to be well described by the rectification model. This was to be expected: the lack of symmetry in the field of the induced current already tells us that a rectification model that takes symmetric conductance as its input cannot describe the asymmetric current induced by this higher applied frequency.

Conductance and induced current as a function of perpendicular field are shown in Figs. 3(a) and 3(b) for different levels of incident power P at 5.56 GHz. Fluctuations in g_{50} decrease with increasing P . In Fig. 3(c), we show the power dependence of the variance

of the conductance. For high applied powers, the variance of conductance fluctuations is reduced to 1/4 of its zero-radiation level. This is expected, since during the fraction of time ($p = 50\%$) that the radiation is on, UCF should be fully suppressed at high power by a combination of shape averaging, dephasing without heating, and heating effects [18,20]. Also shown in Fig. 3(c) is the variance of the extracted “on conductance,” $g_{\text{on}}^{\text{ext}} = 2g_{50} - g_{\text{off}}$, which we observe to decrease at a rate intermediate between $P^{-1/2}$ and P^{-1} at high power. Theory [22] predicts a rate $P^{-1/2}$ in the absence of heating effects.

It is evident in Fig. 3(a) that no significant field asymmetry in conductance is observed, regardless of ac power applied. Recent theory [22] predicts that when applied frequency exceeds the temperature in the leads (which is the case here, $k_B T_e/h \sim 4 \text{ GHz}$), dephasing will lead to field asymmetry in conductance. However, for our experimental conditions the predicted asymmetry is extremely small, smaller in fact than the asymmetry due to drift and noise in our setup (which, as seen in Figs. 1 and 2 is rather small.)

Figure 3(b) shows that mesoscopic fluctuations of the induced current at 5.56 GHz are fully asymmetric in field and increase in amplitude with increasing power. As a measure of this asymmetry, we compare the symmetric and antisymmetric components of current, $I_{s(a)}(B) = [I(B) \pm I(-B)]/2$. Figure 3(d) shows their variances and

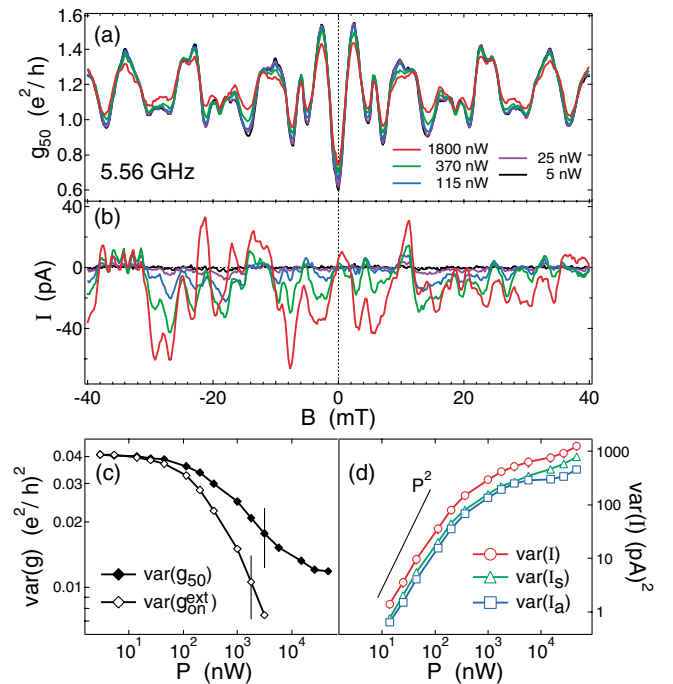


FIG. 3 (color). Magnetic field dependence of (a) conductance and (b) rf-induced dc current, for increasing levels of incident power P at 5.56 GHz. Full sweeps spanned the -100 to $+100 \text{ mT}$ range. (c) Variance of the measured conductance g_{50} and of the extracted on conductance g_{on} , as a function of incident power. (d) Power dependence of the total induced dc current, and of its symmetric and antisymmetric components.

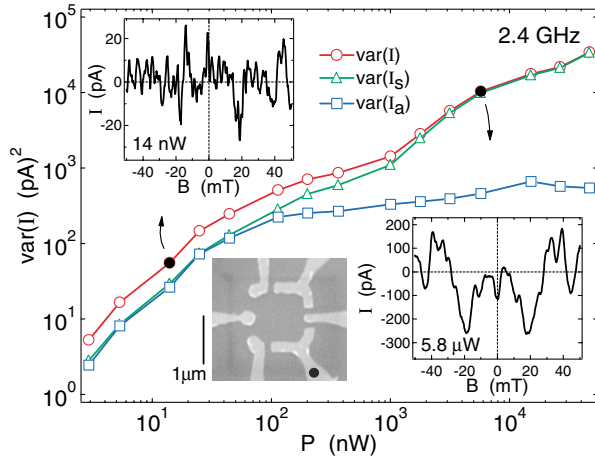


FIG. 4 (color). Variance of symmetric, antisymmetric, and total current (I_s , I_a , I) as functions of incident power P at 2.4 GHz. Upper left inset: Induced current as a function of magnetic field, B , for 14 nW power, showing asymmetric mesoscopic fluctuations with a correlation field ~ 1 mT. Lower right inset: Induced current as a function of magnetic field at $5.8 \mu\text{W}$ power, showing symmetric fluctuations with a correlation field ~ 4 mT. An overall background in this trace was subtracted with a first order polynomial $a_0 + a_1 B$. Lower left inset: Micrograph of device. Dot indicates gate to which ac is applied.

that of total induced current, calculated after subtracting a first order polynomial to $I(B)$ to account for a non-mesoscopic background present at the highest applied powers.

Variances of I_s and I_a are nearly equal, indicating that the current is fully asymmetric for all powers (except at the highest powers, discussed below). Variances of I , I_s , and I_a increase at a rate approaching P^2 at the lowest powers, consistent with theory [21] for the weak pumping limit. The rate weakens at higher incident power, with a crossover near 300 nW, corresponding to an ac gate voltage comparable to the gate-voltage correlation scale.

In the nonadiabatic regime, the induced current is found to range between being predominantly symmetric and fully asymmetric in B , depending on the applied frequency. The degree of symmetry is also found to depend on the applied ac power, with greater symmetry found at higher power. This is illustrated in Fig. 4 for the case of ac gate voltage at 2.4 GHz. At low incident power the current is fully asymmetric, and the fluctuations have a correlation field ~ 1 mT. This is clearly observed in the top left inset, where we show the magnetic field dependence of the induced current for an incident power of 14 nW. At high power, $\text{var}(I_a)$ saturates, leaving a predominantly symmetric signal (Fig. 4, lower inset). The magnetic field correlation scale increases to ~ 4 mT at high power, suggesting enhanced dephasing presumably due to the ac voltages on the gate causing electron heating.

In summary, we use magnetic field symmetry to distinguish mechanisms of induced dc current in response to ac gate voltages in a quantum dot. For lower frequencies,

we find the induced current is symmetric in field, suggesting that mesoscopic rectification is responsible for the induced current in this regime. For higher frequencies (GHz), we find that the induced current can be fully asymmetric in field, suggesting instead that photocurrent can be the dominant source. The qualitative observation of these different regimes, distinguished by field symmetry, is consistent with recent theory [5,7,21].

We thank I. Aleiner, P. Brouwer, V. Falco, A. Johnson, and particularly M. Vavilov for valuable discussion, and thank C.I. Duruöz, S.M. Patel, and S.W. Watson for experimental contributions. We acknowledge support from the NSF under DMR-0072777.

- [1] D. Thouless, Phys. Rev. B **27**, 6083 (1983).
- [2] B. Spivak *et al.*, Phys. Rev. B **51**, 13 226 (1995).
- [3] P.W. Brouwer, Phys. Rev. B **58**, R10135 (1998).
- [4] M. Switkes *et al.*, Science **283**, 1905 (1999).
- [5] T. A. Shutenko *et al.*, Phys. Rev. B **61**, 10366 (2000).
- [6] M. L. Polianski and P.W. Brouwer, Phys. Rev. B **64**, 075304 (2001).
- [7] P.W. Brouwer, Phys. Rev. B **63**, 121303(R) (2001).
- [8] V.I. Falco and D. E. Khmel'nitskii, Zh. Eksp. Teor. Fiz. **95**, 328 (1989) [Sov. Phys. JETP **68**, 186 (1989)].
- [9] A. A. Bykov *et al.*, Pis'ma Zh. Eksp. Teor. Fiz. **49**, 13 (1989) [JETP Lett. **49**, 13 (1989)].
- [10] A. A. Bykov *et al.*, Zh. Eksp. Teor. Fiz. **97**, 1317 (1990) [Sov. Phys. JETP **70**, 742 (1990)].
- [11] J. Liu *et al.*, Phys. Rev. B **45**, 1267 (1992).
- [12] J. J. Lin *et al.*, Phys. Rev. B **45**, 14 231 (1992).
- [13] A. A. Bykov *et al.*, Pis'ma Zh. Eksp. Teor. Fiz. **58**, 538 (1993) [JETP Lett. **58**, 543 (1993)].
- [14] R. E. Bartolo and N. Giordano, Phys. Rev. B **54**, 3571 (1996).
- [15] R. E. Bartolo *et al.*, Phys. Rev. B **55**, 2384 (1997).
- [16] J. Liu and N. Giordano, Phys. Rev. B **39**, 9894 (1989), and references therein.
- [17] A. G. Huibers *et al.*, Phys. Rev. Lett. **83**, 5090 (1999).
- [18] X. B. Wang and V. E. Kravtsov, Phys. Rev. B **64**, 033313 (2001).
- [19] J. J. Lin and J. P. Bird, J. Phys. Condens. Matter **14**, R501 (2002).
- [20] M. G. Vavilov and I. L. Aleiner, Phys. Rev. B **60**, R16311 (1999).
- [21] M. G. Vavilov *et al.*, Phys. Rev. B **63**, 195313 (2001).
- [22] M. G. Vavilov and I. L. Aleiner, Phys. Rev. B **64**, 085115 (2001).
- [23] M. Moskalets and M. Büttiker, Phys. Rev. B **66**, 205320 (2002); Sang Wook Kim, Phys. Rev. B **66**, 235304 (2002).
- [24] M. Switkes, Ph.D. thesis, Stanford University, 1999 (available at <http://marcuslab.harvard.edu>).
- [25] L. P. Kouwenhoven *et al.*, in *Mesoscopic Electron Transport*, edited by L. L. Sohn, L. P. Kouwenhoven, and G. Schön (Kluwer, Dordrecht, 1997).
- [26] The magnetic field correlation field B_c is extracted from the slope of the log-power spectrum of magnetic field conductance fluctuations, $S(f) = S(0)e^{-2\pi B_c f}$. See A. G. Huibers *et al.*, Phys. Rev. Lett. **81**, 200 (1998).